

1 **Air-sea exchange and gas-particle partitioning of polycyclic aromatic hydrocarbons in**  
2 **the Mediterranean**

3 Marie D. Mulder<sup>a</sup>, Angelika Heil<sup>b</sup>, Petr Kukučka<sup>a</sup>, Jana Klánová<sup>a</sup>, Jan Kuta<sup>a</sup>, Roman Prokeš<sup>a</sup>,  
4 Francesca Sprovieri<sup>c</sup>, Gerhard Lammel<sup>a,d\*</sup>

5 <sup>a</sup> Masaryk University, Research Centre for Toxic Compounds in the Environment, Brno,  
6 Czech Republic

7 <sup>b</sup> Helmholtz Research Centre Jülich, Institute for Energy & Climate Research, Jülich,  
8 Germany

9 <sup>c</sup> CNR, Institute for Atmospheric Pollution Research, Rende, Italy

10 <sup>d</sup> Max Planck Institute for Chemistry, Mainz, Germany

11 \* phone +420-54949-4106, fax +420-54949-2840, lammel@recetox.muni.cz

12

13 **Abstract**

14 Polycyclic aromatic hydrocarbons concentration in air of the central and eastern  
15 Mediterranean in summer 2010 was 1.45 (0.30-3.25) ng m<sup>-3</sup> (sum of 25 PAHs), with 8 (1-17)  
16 % in the particulate phase, almost exclusively associated with particles <0.25 µm. The total  
17 deposition flux of particulate PAHs was 0.35-0.80 µg m<sup>-2</sup> year<sup>-1</sup>. The diffusive air-sea  
18 exchange fluxes of fluoranthene and pyrene were mostly found net-depositional or close to  
19 phase equilibrium, while retene was net-volatilisation in a large sea region. Regional fire  
20 activity records in combination with box model simulations suggest that seasonal  
21 depositional input of retene from biomass burning into the surface waters during summer is  
22 followed by an annual reversal of air-sea exchange, while inter-annual variability is  
23 dominated by the variability of the fire season. One third of primary retene sources to the sea

24 region in the period 2005-2010 returned to the atmosphere as secondary emissions from  
25 surface seawaters. It is concluded that future negative emission trends or interannual  
26 variability of regional sources may trigger the sea to become a secondary PAH source through  
27 reversal of diffusive air-sea exchange.

28

29 **Capsule:** Polycyclic aromatic hydrocarbons phase distributions in marine aerosols, direction  
30 of air-sea exchange and open fires as a possible source characterised in the Mediterranean

31

32 **Keywords:** polycyclic aromatic hydrocarbons, long-range transport, air-sea exchange, open  
33 fires

34

## 35 **1. Introduction**

36 The marine atmospheric environment is a receptor for polycyclic aromatic hydrocarbons  
37 (PAHs) which are advected from combustion sources on land (power plants, biomass  
38 burning, road transport, domestic heating). Marine sources may be significant near transport  
39 routes (ship exhaust). Long-range transport from urban and industrial sources on land are the  
40 predominant sources of PAHs in the Mediterranean (Masclet et al., 1988; Tsapakis et. al,  
41 2003 and 2006; Tsapakis and Stephanou, 2005a). A number of PAHs are semivolatile (vapour  
42 pressures at 298 K in the range  $10^{-6}$ - $10^{-2}$  Pa) and, hence partition between the gas and  
43 particulate phases of the atmospheric aerosol, influenced by temperature, particulate phase  
44 chemical composition and particle size (Keyte et al., 2013). Upon deposition to surface water  
45 PAHs partition between the aqueous and particulate (colloidal and sinking) phases and may  
46 bioaccumulate in marine food chains (Lipiatou and Saliot, 1991; Dachs et al., 1997; Tsapakis

47 et. al, 2003; Berrojalbiz et al., 2011). They were also found enriched in the sea-surface  
48 microlayer relative to subsurface water (Lim et al., 2007; Guitart et al., 2010). Semivolatile  
49 PAHs may be subject to re-volatilisation from the sea surface (reversal of air-sea exchange),  
50 similar to chlorinated semivolatile organics (Bidleman and McConnell, 1995), in case high  
51 concentrations in surface water would build up. This had been predicted by  
52 multicompartamental modelling for 2-4 ring PAHs for polluted coastal waters and also the  
53 open ocean (Greenfield and Davis, 2005; Lammel et al., 2009a) and was indeed observed in  
54 coastal waters off the northeastern United States (Lohmann et al., 2011). Field studies in the  
55 open sea found net-deposition to prevail whenever determined (e.g. Tsapakis et al., 2006;  
56 Balasubramanian and He, 2010; Guitart et al., 2010; Castro-Jiménez et al., 2012; Mai, 2012).  
57 However, some 3-4 ring parent PAHs, among them fluorene (FLU), fluoranthene (FLT) and  
58 pyrene (PYR), were reported to be close to phase equilibrium in the Mediterranean, Black  
59 and North seas (Castro-Jiménez et al., 2012; Mai, 2012), and net volatilisation of FLT and  
60 PYR was observed in the open southeastern Mediterranean Sea in spring 2007 (Castro-  
61 Jiménez et al., 2012).

62 The aim of the measurements on board RV Urania was to investigate levels of organic  
63 pollutants in summer in Mediterranean air and gain insights about sources and phase  
64 partitioning in the aerosol of these substances. This study is on the cycling of PAHs in the  
65 marine atmosphere.

66

## 67 **2. Methods**

### 68 **2.1 Sampling**

69 Samples were taken during the RV Urania cruise, 27 August – 12 September 2010 (see  
70 Supplementary Material (SM), Fig. S1). PAHs were collected in the gaseous and particulate  
71 phases using high volume samplers (Digitel) equipped with one glass fibre filter (Whatman)  
72 and one polyurethane foam (PUF) plug (Gumotex Břeclav, density 0.030 g cm<sup>-3</sup>, 50 mm  
73 diameter, cleaned by extraction in acetone and dichloromethane, 8 h each, placed in a glass  
74 cartridge) in series. Particle size was classified in the particulate phase using high-volume  
75 filter sampling ( $F = 68 \text{ m}^3 \text{ h}^{-1}$ , model HVS110, Baghirra, Prague) and low-volume impactor  
76 sampling ( $F = 0.54 \text{ m}^3 \text{ h}^{-1}$ , Sioutas 5-stage cascade, PM<sub>10</sub> inlet, cutoffs 2.5, 1.0, 0.5, 0.25  $\mu\text{m}$   
77 of aerodynamic particle size and back-up filter, impaction on quartz fibre filters (QFF), SKC  
78 Inc., Eighty Four, USA, sampler Baghirra PM<sub>10-35</sub>). In total 15 high-volume filter samples,  
79 exposed 8-36 h (230-1060 m<sup>3</sup> of air), and 3 low-volume impactor samples, exposed 5 d, were  
80 collected. Water sampling was performed using the stainless steel ROSETTE active sampling  
81 device equipped with 24 Niskin bottles (volume of 10 l) deployed in water at 1.5 m depth for  
82 surface water sampling.

83

84 PAH sampling on GFF and in PUF can be subject to losses related to oxidation of sorbed  
85 PAH by ozone (Tsapakis and Stephanou, 2003). This artifact is species-specific and the more  
86 pronounced the higher the ozone concentration and the longer the sampling time. Among the  
87 PAHs addressed benzo(a)pyrene and pyrene have been identified as particularly vulnerable to  
88 oxidation. Based on such sampling artefact quantification studies (Tsapakis and Stephanou,  
89 2003; Galarneau et al., 2006) and ozone levels (Table 1a) and sampling times (Table S1) we  
90 expect that total PAHs are underestimated by up to 50% in the gas-phase and by up to 25% in  
91 the particulate phase.

92 With the aim to characterize the potential influences of ship-bourne emissions on the  
93 samples, passive air samplers with PUF disks were exposed at 5 different locations on board  
94 during 16 days. The PAH levels of these samples indicated that ship-based contamination was  
95 negligible.

96

## 97 **2.2 PAHs analyses and quality assurance**

98 For PAH analysis all samples were extracted with dichloromethane in an automatic extractor  
99 (Büchi B-811). Surrogate recovery standards (D8-naphthalene, D10-phenanthrene, D12-  
100 perylene) were spiked on each PUF and GFF prior to extraction. The volume was reduced  
101 after extraction under a gentle nitrogen stream at ambient temperature, and fractionation  
102 achieved on a silica gel column.

103 The first portion of the extract was fractionated on a silica column (5 g of silica 0.063 – 0.200  
104 mm, activated 12 h at 150°C). The first fraction (10 mL n-hexane) containing aliphatic  
105 hydrocarbons was discarded. The second fraction (20 mL DCM) containing PAHs was  
106 collected and then reduced by stream of nitrogen in a TurboVap II (Caliper LifeSciences,  
107 USA) concentrator unit and transferred into an insert in a vial. Terphenyl was used as syringe  
108 standard, final volume was 200 µL. GC-MS analysis was performed on a 6890N GC  
109 equipped with a 60m x 0.25mm x 0.25µm DB5-MS column (Agilent J&W, USA) coupled to  
110 5973N MS (Agilent, USA). The MS was operated in EI+ mode with selected ion recording  
111 (SIR).The targeted compounds are the 16 EPA priority PAHs (i.e., naphthalene (NAP),  
112 acenaphthylene (ACY), acenaphthene (ACE), fluorene (FLN), phenanthrene (PHE),  
113 anthracene (ANT), fluoranthene (FLT), pyrene (PYR), benzo(a)anthracene (BAA), chrysene  
114 (CHR), benzo(b)fluoranthene (BBF), benzo(k)fluoranthene (BKF), benzo(a)pyrene (BAP),

115 indeno(123cd)pyrene (IPY), dibenzo(ah)anthracene (DBA), benzo(ghi)perylene (BPE)), 10  
116 more parent PAHs (i.e., benzo(ghi)fluoranthene (BGF), cyclopenta(cd)pyrene (CPP),  
117 triphenylene (TPH), benzo(j)fluoranthene (BJF), benzo(k)fluoranthene (BKF),  
118 benzo(e)pyrene (BEP), perylene (PER), dibenz(ac)anthracene (DCA), anthranthrene (ATT),  
119 and coronene (COR)), and one alkylated PAH, retene (RET). The injection volume was 1  $\mu$ L.  
120 Terphenyl was used as internal standard.

121 Field blank values,  $b$ , were gained from GFFs and PUFs manipulated in the field, as far as  
122 possible identical to the samples, except without switching the high-volume sampler on. No  
123 QFF field blank was taken for impactor sampling. As no PAHs were detected in the stages  
124 corresponding to 2.5-10  $\mu$ m (all PAHs < limit of detection in all such samples), instead the  
125 mean of values of the QFF substrates of the 2 uppermost impactor stages (in total 6) was  
126 taken. The respective  $b$  value was subtracted from sample values. The limit of quantification  
127 needs to take the accuracy of the blank level into account. In lack of a measure for the  
128 variation of the field blank, the relative standard deviation (SD) of field blanks from earlier  
129 field campaigns,  $(\sigma_c/b_c)$ , on a high-mountain site (high-volume sampling summer 2007,  $n = 5$ ;  
130 Lammel et al., 2009b) and in the Mediterranean (impactor sampling summer 2008,  $n = 6$ ;  
131 Lammel et al., 2010a) was used ( $\sigma = (\sigma_c/b_c) \times b$ ). The identical samplers, sampling and  
132 analysis protocols for all analytes had been applied. Values below the sum of the field blank  
133 value (from this campaign) and 3 relative SDs of the field blank values (from the previous  
134 campaigns) were considered <LOQ ( $LOQ = b + 3\sigma$ ). NAP and ACY were excluded from the  
135 data set, because of the lack of blank values. The field blank values of most other analytes  
136 were below instrument LOQ in high-volume PUF and GFF samples. However, higher field  
137 LOQs, up to (6-25)  $\text{pg m}^{-3}$  (according to sampled volume of air) resulted for ANT, PYR and

138 RET, and up to (45-180)  $\text{pg m}^{-3}$  for ACE, FLN, PHE and FLT in PUF. Field LOQs of PAHs in  
139 impactor QFF samples were below instrumental LOQ for most substances, but in the range  
140 (8-15)  $\text{pg m}^{-3}$  for ACE, ANT, and FLT,  $\approx 55 \text{ pg m}^{-3}$  for FLN, and 120-140  $\text{pg m}^{-3}$  for NAP and  
141 PHE.

142 The instrument limit of quantification (LOQ), which is based on the lowest concentration of  
143 calibration standards used, was 0.5 ng, corresponding to 0.5-2.5  $\text{pg m}^{-3}$  for high-volume  
144 samples,  $\approx 8 \text{ pg m}^{-3}$  for impactor samples, 6-10  $\text{pg m}^{-3}$  for semivolatile PAHs determined in  
145 passive air samples and up to 200  $\text{pg m}^{-3}$  for non volatile PAHs in passive air samples.

146 Water samples (2-2.5 L) were extracted immediately after their collection using solid phase  
147 extraction on  $\text{C}_{18}$  Empore discs using a vacuum manifold device. Disks were stored closed in  
148 glass vials in a freezer and transported to the processing laboratory, PAHs were eluted from  
149 disks using 40 mL of dichloromethane. The above listed PAHs were analysed on GC/MS  
150 (Agilent GC 6890N coupled to an Agilent single quadrupole MS 5973N operating in electron  
151 impact ionisation mode). LOQ was  $0.1 \text{ ng L}^{-1}$ .

152

### 153 **Other trace constituents and meteorological parameters**

154 Ozone was measured with an absorption method (Teledyne-API model 400A UV) on the top  
155 deck (10 m above sea surface). Meteorological parameters (air temperature, humidity, wind  
156 direction and velocity) and oceanographic parameters were determined aboard.

157

### 158 **2.3 Models of gas-particle partitioning**

159 The data set (15 high-volume samples of separate gas and particulate phase concentrations) is  
160 used to test gas-particle partitioning models for semivolatile organics in terms of the organics'

161 mass size distribution and size dependent particulate matter (PM) composition. The models  
162 assume different processes to determine gas-particle partitioning, i.e. an adsorption model  
163 (Junge-Pankow; Pankow, 1987), and two absorption models (i.e.  $K_{OA}$  models; Finizio et al.,  
164 1997; Harner and Bidleman, 1998). Absorption is into particulate OM. Adsorption to soot is a  
165 significant gas---particle partitioning processes for PAHs, but no soot data or PM chemical  
166 composition data are available. We, therefore, refrain from testing dual adsorption and  
167 absorption models (e.g. Lohmann and Lammel, 2004). Particulate mass fraction,  $\theta$ , and  
168 partitioning coefficient,  $K_p$ , are defined by the concentrations in the 2 phases:

169

$$170 \quad \theta = c_p / (c_p + c_g)$$

171

$$172 \quad K_p = c_p / (c_g \times c_{TSP}) = \theta / [(1 - \theta) \times c_{TSP}]$$

173

174 with  $c_p$  and  $c_g$  in units of  $\text{ng m}^{-3}$ ,  $c_p$  representing the whole particle size spectrum.

175 Different models describe different processes to quantify differences in ad- and absorption  
176 between compounds. The Junge-Pankow model uses the vapour pressure of the subcooled  
177 liquid  $p_L^0$ ,  $\theta = c_j S / (p_L^0 + c_j S)$ , (data taken from Lei et al., 2002),  $c_j$  should be approximately  
178 171 Pa cm for PAHs ( Pankow, 1987). The aerosol particle surface,  $S$ , was not measured and  
179 a typical value for maritime aerosols is adopted instead ( $4.32 \times 10^{-7} \text{ cm}^{-1}$ ; Jaenicke, 1988).  
180 Harner and Bidleman, 1998, use the  $\log K_{OA}$  and  $f_{OM}$ :  $\log K_p = \log K_{OA} + \log f_{OM} - 11.91$ ; and  
181 Finizio et al., 1997, uses only the  $K_{OA}$  as predictor (data taken from Ma et al., 2010):  $\log K_p =$   
182  $0.79 \times \log K_{OA} - 10.01$ . The range of the fraction of OM used here is based on Putaud et al.,  
183 2004 (16% lower limit) and Spindler et al., 2012 (45% upper limit).

184

## 185 **2.4 Air-sea diffusive mass exchange calculations**

186 State of phase equilibrium is addressed by fugacity calculation, based on the Whitman two-  
187 film model (Liss and Slater, 1974; Bidleman and McConnell, 1995). The fugacity ratio (FR)  
188 is calculated as:

189

$$190 \text{ FR} = f_a/f_w = C_aRT_a / (C_wH_{\text{Tw,salt}})$$

191

192 with gas-phase concentration  $C_a$  ( $\text{ng m}^3$ ), dissolved aqueous concentration  $C_w$  ( $\text{ng m}^3$ ),  
193 universal gas constant  $R$  ( $\text{Pa m}^3 \text{ mol}^{-1} \text{ K}^{-1}$ ), water temperature and salinity corrected Henry's  
194 law constant  $H_{\text{Tw,salt}}$  ( $\text{Pa m}^3 \text{ mol}^{-1}$ ), and air temperature  $T_a$  (K).  $C_w$  is derived from the bulk  
195 seawater concentration:

196

$$197 C_w = C_{\text{bulk}} / (1 + K_{\text{POC}} C_{\text{POC}} + K_{\text{DOC}} C_{\text{DOC}})$$

198

199 with  $C_{\text{POC}}$  and  $C_{\text{DOC}}$  from Pujó-Pay et al., 2011,  $K_{\text{POC}}$  and  $K_{\text{DOC}}$  from Karickhoff et al, 1981,  
200 Lüers and ten Hulscher 1996, Rowe et al, 2009, and Ma et al, 2010. Values  $0.3 < \text{FR} < 3.0$  are  
201 conservatively considered to not safely differ from phase equilibrium, as propagating from  
202 the uncertainty of the Henry's law constant,  $H_{\text{Tw,salt}}$ , and measured concentrations (e.g., Bruhn  
203 et al., 2003; Castro-Jiménez et al., 2012; Zhong et al., 2012). This conservative uncertainty  
204 margin is also adopted here, while  $\text{FR} > 3.0$  indicates net deposition and  $\text{FR} < 0.3$  net  
205 volatilisation. The diffusive air–seawater gas exchange flux ( $F_{\text{aw}}$ ,  $\text{ng m}^{-2} \text{ day}^{-1}$ ) is calculated

206 according to the Whitman two-film model (Bidleman and McConnell, 1995; Schwarzenbach  
207 et al., 2003):

208

$$209 \quad F_{aw} = k_{ol} (C_w - C_a RT_a / H_{Tw,salt})$$

210

211 with air-water gas exchange mass transfer coefficient  $k_{ol}$  ( $\text{m h}^{-1}$ ), accounting for resistances to  
212 mass transfer in both water ( $k_w$ ,  $\text{m h}^{-1}$ ) and air ( $k_a$ ,  $\text{m h}^{-1}$ ), defined as

213

$$214 \quad 1/k_{ol} = 1/k_w + RT_a / (k_a H_{Tw,salt})$$

215

216 with  $k_a = (0.2U_{10} + 0.3) * (D_{i,air} / D_{H_2O,air})^{0.61} \times 36$ ,  $k_w = (0.45U_{10}^{1.64}) \times (Sc_i / Sc_{CO_2})^{-0.5} \times 0.01$ .  $U_{10}$

217 is the wind speed at 10 meter height above sea level ( $\text{m s}^{-1}$ ),  $D_{i,air}$  and  $D_{H_2O,air}$  are the

218 temperature dependent diffusivities of substance  $i$  and  $\text{H}_2\text{O}$  in air, and  $Sc_i$  and  $Sc_{CO_2}$  are the

219 Schmidt numbers for substance  $i$  and  $\text{CO}_2$  (see Bidleman and McConnell, 1995; Zhong et al.

220 2012; and references therein).  $U_{10}$ ,  $T_a$ ,  $T_w$  and air pressure are taken from the ship based

221 measurements.

## 222 **2.5 Non-steady state 2-box model**

223 The air–sea mass exchange flux of RET is simulated by a non-steady state zero-dimensional

224 model of intercompartmental mass exchange (Lammel, 2004). RET is selected, because of

225 the prevalence of one dominating source. This 2-box model predicts concentrations by

226 integration of two coupled ordinary differential equations that solve the mass balances for the

227 two compartments, namely the atmospheric marine boundary layer (MBL) and seawater

228 surface mixed layer. Processes considered in air are dry (particle) deposition, removal from

229 air by reaction with the hydroxyl radical, and air-sea mass exchange flux (dry gaseous  
230 deposition), while in seawater export (settling) velocity, deposition flux from air, air-sea mass  
231 exchange flux (volatilisation), and degradation (as 1<sup>st</sup> order process) are considered. All input  
232 parameters are listed in the SM, Table S2.

233 Atmospheric depositions related to emissions from open fires are assumed to provide the  
234 only source for seawater RET. These are available as daily time series for the East  
235 Mediterranean domain (28-45°N, 8-30°E) through the fire-related PM<sub>2.5</sub> emissions as  
236 provided by the Global Fire Assimilation System (GFASv1.0; Kaiser et al., 2012) in  
237 combination with an emission factor (207 mg RET in PM<sub>2.5</sub> (kg fuel burnt)<sup>-1</sup>; Schmidl et al.,  
238 2008). The fire emissions are averaged over the domain and assumed to disperse within the  
239 MBL only. This is justified due to the assumed underestimation of the fire related emissions  
240 and ignorance of other (emission) sources. The 2-box model is run for the years 2005-2010,  
241 for the east Mediterranean domain (28-45°N, 8-30°E) with a 1 h time resolution. Fluxes in  
242 the range  $F_{em} = (0.30 \pm 1.46) \text{ ng m}^{-2} \text{ h}^{-1}$  (positive defined upward) are simulated (using the  
243 initially estimated parameter set, Table S2). GFAS uses global satellite observations of fire  
244 radiative power to estimate daily dry matter combustion rates and fire emission fluxes. The  
245 GFAS system partly corrects for observational gaps (e.g. due to cloud cover) and detects fires  
246 in all biomes, except for very small fires (lower detection limit of around 100-1000 m<sup>2</sup>  
247 effective fire area).

248

## 249 **2.6 Analysis of long-range advection of air**

250 Distributions of potential sources can be identified by inverse modelling using meteorological  
251 input data (Stohl et al., 2003; Eckhardt et al., 2007). So-called retroplumes are generated

252 using operational weather prediction model data and a Lagrangian particle dispersion model,  
253 FLEXPART (Stohl et al., 1998, 2005). Hereby, 50000 virtual particles per hour were  
254 'released' and followed backwards in time for 5 days. The model output is a 3-D distribution  
255 of residence time.

256

### 257 **3. Results and discussion**

#### 258 **3.1 PAH concentrations in air and seawater**

259 The mean total (i.e., sum of gaseous and particulate)  $\Sigma 25$  PAHs concentration is  $1.45 \text{ ng m}^{-3}$   
260 (time-weighted;  $1.54$  with values  $< \text{LOQ}$  replaced by  $\text{LOQ}/2$ , see Table 1a), and ranged from  
261  $0.30\text{-}3.25 \text{ ng m}^{-3}$ . The spatial variability of PAH levels in the Mediterranean is large,  
262 determined by long-range advection (Tsapakis and Stephanou, 2005a; Tsapakis et al., 2006).  
263 The levels found in this study in the southeastern Mediterranean are for most substances  
264 lower than found earlier (Table 2). In the ISS some PAHs are found somewhat higher than  
265 previously measured i.e., FLT and PYR (in the gas-phase) and BAP and PER (in the  
266 particulate phase). Due to a sampling artefact BAP and other particulate phase PAHs could be  
267 underestimated by up to 25% (aforementioned, section 2.1). The seasonality of emissions and  
268 the variability of advection or advection in combination with different cruise routes being  
269 influenced differently by coastal or ship emission plumes can have a large influence and may  
270 explain these differences. On the other hand, the duration of temporal averaging atmospheric  
271 concentrations was similar across the various studies. Diagnostic ratios ( $\text{BAA}/(\text{BAA}+\text{CHR})$ ,  
272  $\text{FLT}/(\text{FLT}+\text{PYR})$ ; Dvorská et al., 2011) in some of the samples (No. 2, 4, 7, 8, and 15) reflect  
273 the influence of traffic and industrial sources. We investigated the potential source  
274 distribution of individual samples collected along the cruise (section 2.6) and found that

275 indeed maxima of PAH concentrations corresponded with air masses having resided over  
 276 large urban areas, and, vice versa, low concentrations corresponded with air masses without  
 277 apparent passage of such areas (illustrated in Fig. S5). This finding is supported by the ozone  
 278 data i.e., 53 (47-65) ppbv during influence from urban areas but 37 (33-62) ppbv otherwise.  
 279 It had been pointed out that the source distribution around the Mediterranean may cause a  
 280 west-east gradient, leading to higher concentrations found in the Ionian Sea and Sicily region  
 281 (ISS) than in the southeastern Mediterranean (SEM; Berrojalbiz et al., 2011). This gradient is  
 282 somewhat reflected in our results, as levels in the ISS exceeded levels in the SEM (Table 2a).  
 283 Most PAH concentrations in surface seawater were <LOQ, while FLT, PYR and RET were  
 284 quantified in at least part of the samples (Table 1b). These observed seawater contamination  
 285 levels are comparable to levels found in the region 2 and 1 decades ago (Lipiatou et al., 1997;  
 286 Tsapakis et al., 2003). The concentrations near Crete (samples No. 7 and 8a) are very similar  
 287 to those found in fall 2001 and winter-spring 2002 (Tsapakis et al., 2006; FLT = 0.15 (0.11-  
 288 0.21) ng L<sup>-1</sup> , PYR = 0.12 (0.07-0.17) ng L<sup>-1</sup>).

289

290 Table 1. Concentrations of PAHs found in (a.) air (total, i.e. sum of gas and particulate  
 291 phases, ng m<sup>-3</sup>) and (b.) seawater (total, i.e. sum of dissolved and particulate, ng L<sup>-1</sup>) as time-  
 292 weighted mean (min-max). n<sub>LOQ</sub> = number of samples > LOQ (out of 15 air and 23 seawater  
 293 samples). PAHs with concentrations <LOQ in all samples not listed. For calculation of mean  
 294 values <LOQ were replaced by LOQ/2. Ozone levels are given, too (ppbv).

295 a)

	n <sub>LOQ</sub>	mean (min-max)
--	------------------	----------------

ACE	4	0.025 (<0.020–0.089)
FLN	10	0.137 (<0.030–0.396)
PHE	15	0.581 (0.144–1.41)
ANT	13	0.043 (0.008–0.22)
RET	14	0.016 (0.006–0.030)
FLT	15	0.262 (0.053–0.795)
PYR	15	0.203 (0.044–0.564)
BAA	15	0.01 (0.0014–0.031)
CHR	15	0.04 (0.012–0.092)
TPH	15	0.018 (0.007–0.032)
BBN	11	0.018 (0.001–<0.085)
BBF	15	0.021 (0.004–0.102)
BKF	14	0.012 (0.002–<0.085)
BAP	12	0.015 (0.001–<0.085)
BGF	15	0.021 (0.005–0.067)
CPP	7	0.012 (0.001–<0.085)
BJF	15	0.016 (0.002–0.079)
BEP	14	0.019 (0.004–0.088)
PER	7	0.012 (0.001–0.1)
IPY	7	0.022 (0.008–0.094)
BPE	6	0.02 (0.009–0.085)
COR	5	0.016 (0.002–0.1)

Σ25 PAHs		1.539 (0.44–4.694)
Ozone		42 (33 – 65)

296

297 b)

	n <sub>LOQ</sub>	mean (min-max)
PHE	1	1.1
RET	12	0.1 (<0.1–0.5)
FLT	10	0.1 (<0.1–0.3)
PYR	7	0.2 (<0.2–0.9)

298

299 Table 2 Gaseous (a) and particulate (b) concentrations in air (time-weighted mean (min-max),  
300 ng m<sup>-3</sup>) of selected PAH compared to other studies in the Ionian Sea and Sicily region (ISS)  
301 and in the southeastern Mediterranean (SEM). For calculation of means values <LOQ were  
302 replaced by LOQ/2. RV = research vessel cruise.

303 a)

	ISS		SEM			
	RV August- September 2010	RV June 2006, May 2007	RV August- September 2010	RV June 2006, May 2007	Finokalia September- October 2001, February, March and July 2002 <sup>(1)</sup>	Finokalia November 2000- February 2002 <sup>(2)</sup>
	this study	Castro- Jiménez 2012	this study	Castro-Jiménez 2012	Tsapakis et al. 2006	Tsapakis & Stephanou 2005

FLN	0.18 (0.050– 0.40)	2.25 (1.27– 5.65)	0.11 (<0.027– 0.34)	0.69 (0.36– 1.23)	1.05 (0.15– 1.67)	1.8 (0.2–5.7)
PHE	0.59 (0.14– 1.10)	7.00 (3.52– 15.45)	0.51 (0.14– 1.41)	3.94 (2.50– 6.35)	4.78 (1.75– 7.78)	7.3 (1.5–27.7)
ANT	0.064 (<0.021– 0.10)	0.37 (0.18– 0.55)	0.067 (<0.013– 0.22)	0.20 (0.16– 0.30)	0.61 (0.12– 1.31)	0.9 (0.1–4.5)
FLT	0.15 (0.053– 0.31)	0.05 (0.02– 0.07)	0.15 (0.061– 0.37)	0.007 (0.003– 0.011)	0.82 (0.12– 1.69)	1.8 (0.07–6.0)
PYR	0.15 (0.044– 0.29)	0.04 (0.02– 0.06)	0.19 (0.058– 0.56)	0.006 (0.003– 0.009)	0.65 (0.14– 0.97)	0.9 (0.1–2.8)
CHR	0.013 (0.0071– 0.021)	0.09 (0.03– 0.23)	0.018 (0.012– 0.037)	0.03 (0.02– 0.05)	0.18 (0.06– 0.33)	0.2 (<0.001–0.6)
Sum of 6 PAHs	1.1	9.8	1.0	4.9	8.1	12.9

304

305 b)

	ISS		SEM		
	RV August- September 2010	RV June 2006, May 2007	RV August- September 2010	RV June 2006, May 2007	Finokalia November 2000- February 2002
	this study	Castro-Jiménez 2012	this study	Castro- Jiménez 2012	Tsapakis & Stephanou 2005

FLN	<0.92 (<0.60– <1.1)	0.001 (0.0009– 0.002)	<0.66 (<0.33– <1.4)	0.0013 (0.0011– 0.0016)	0.02 (<0.001– 0.01)
PHE	<1.9 (<1.2– <2.3)	0.06 (0.01– 0.12)	<1.6 (<0.66– <2.7)	0.04 (0.01– 0.13)	0.05 (0.004–0.2)
ANT	<0.21 (<0.14– <0.26)	0.007 (0.0009– 0.012)	<0.16 (<0.07– <0.32)	0.009 (0.0007– 0.023)	0.004 (<0.001– 0.02)
FLT	<0.85 (<0.56– <1.0)	0.099 (0.01– 0.19)	<0.62 (<0.30– <1.3)	0.049 (0.01– 0.12)	0.1 (0.04–0.2)
PYR	<0.11 (<0.070– <0.13)	0.109 (0.016– 0.216)	<0.08 (<0.044– <0.16)	0.057 (0.012– 0.142)	0.04 (0.01–0.01)
BAA	0.0065 (<0.0018– 0.025)	0.013 (0.006– 0.023)	0.0030 (<0.0006– 0.0080)	0.018 (0.004– 0.046)	0.03 (0.003–0.1)
CHR	0.021 (0.0030– 0.076)	0.04 (0.01– 0.08)	0.010 (0.0033– 0.020)	0.043 (0.012– 0.101)	0.1 (0.02–0.3)
BBF	0.028 (<0.0018– 0.010)	0.029 (0.012– 0.045)	0.014 (0.0042– 0.033)	0.033 (0.010– 0.060)	0.04 (<0.001–0.2)
BKF	0.015 (<0.0018– 0.057)	0.015 (0.005– 0.027)	0.0065 (0.0018– 0.015)	0.089 (0.005– 0.333)	0.04 (<0.001–0.2)

BAP	0.016 (<0.0009– 0.072)	0.009 (0.04– 0.016)	0.0052 (<0.0011– 0.0098)	0.034 (0.005– 0.081)	0.02 (0.01–0.05)
BJF	0.021 (<0.0018– 0.079)	0.015 (0.014– 0.016)	0.011 (0.0023– 0.031)	0.010 (0.008– 0.011)	-
BEP	0.023 (<0.0018– 0.088)	0.03 (0.02– 0.05)	0.011 (0.0035– 0.025)	0.046 (0.017– 0.093)	0.04 (0.01–0.1)
PER	0.0028 (<0.00096 –0.011)	0.002 (0.0005– 0.004)	0.00085 (<0.0006– 0.0021)	0.026 (0.0001– 0.068)	0.004 (<0.001– 0.01)
IPY	0.020 (<0.00096 –0.094)	0.018 (0.006– 0.032)	0.0043 (<0.00052– 0.019)	0.009 (0.002– 0.013)	0.03 (0.009–0.2)
BPE	<0.0014 (<0.00096 –0.0018)	0.026 (0.017– 0.042)	0.0067 (<0.00052– 0.020)	0.081 (0.012– 0.210)	0.03 (0.010–0.09)
Sum of 15 PAHs	0.15	1.06	0.06	0.54	0.54

306 <sup>(1)</sup> months Sep and Oct 2001, Feb, Apr and May 2002. No particulate data reported.

307 <sup>(2)</sup> 24h per month between Feb 2000 and Feb 2002

308

309 **3.2 Gas-particle partitioning**

310 Only a small mass fraction of the total,  $\theta = 0.08$ , is found in the particulate phase, confirming  
311 earlier findings from remote sites in the region (Tsapakis and Stephanou, 2005a; Tsapakis et  
312 al., 2006; Table 3c). The particulate mass fraction,  $\theta$ , of four semivolatile PAHs varied  
313 considerably along track (see SM Fig. S2).  $\theta$  is thought to be strongly influenced by  
314 temperature and doubling per 13 K cooling was found in a Mediterranean environment  
315 (Lammel et al., 2010b) apart from PM composition. We refrain from an exploration of the  
316 vapour pressure ( $p_{L0}$ ) dependence of  $\theta$  (or  $K_p$ ): a low time resolution implies lack of  
317 representativeness of the temperature measurement for the phase change (Pankow and  
318 Bidleman, 1992), non-equilibrium conditions cannot be excluded (but are likely as a  
319 consequence of time resolution; Hoff et al., 1998) and supporting physical and chemical  
320 aerosol parameters, necessary to relate are lacking.

321 of only little temperature variation during the cruise ( $T_{\text{mean\_sample}} = 21\text{-}27^\circ\text{C}$ , Fig. S2). For  
322 similar temperatures higher  $\theta$  values had been observed at sites on the region influenced by  
323 urban and industrial sources (Mandalakis et al., 2002; Tsapakis and Stephanou, 2005b; Akyüz  
324 and Cabuk, 2010), which is probably related to the influence of higher organic and soot PM  
325 mass fractions. Gas-particle partitioning models (Table 3) underpredict  $\theta$ , except the Finizio  
326 et al., 1997, model for one substance, TPH.  $\theta$  predicted by the Junge-Pankow (JP) model  
327 comes closest. A number of semivolatile PAHs could not be included in this test of gas-  
328 particle partitioning models as concentrations in either the gas-phase (CPP, BBF, BJF), or the  
329 particulate phase (FLT, PYR, BBN) did not exceed LOQ or no insufficient input data were  
330 available (BBF). The neglect of adsorption to soot, not covered by the gas-particle  
331 partitioning models tested, may explain at least part of the underprediction (Lohmann and  
332 Lammel, 2004). Due to the lack of OC/EC data an extended examination is not possible.

333 In size-segregated samples particulate PAH mass was almost exclusively found in the size  
 334 fraction <0.25  $\mu\text{m}$  a.e.d. (<LOQ in the other stages, except 0.002  $\text{ng m}^{-3}$  CPP in the size  
 335 fraction corresponding to 0.5-1.0  $\mu\text{m}$ ; S2.1, Table S4). Most particulate phase PAHs, 40%,  
 336 have been found associated with particles <0.5 $\mu\text{m}$  out of 5 size ranges in the marine  
 337 background aerosol of the sea region (coast of Crete, November 1996 – June 1997; Kavouras  
 338 and Stephanou, 2002). At continental sites in central and southern Europe mass median  
 339 diameters of PAHs were found to be in the accumulation range, mostly 0.5-1.4  $\mu\text{m}$  (Schnelle  
 340 et al., 1995; Kiss et al., 1998; Lammel et al., 2010b and 2010c), but also a second, coarse  
 341 mode was found (up to 2.4  $\mu\text{m}$ ; Chrysikou et al., 2009).

342

343 Table 3. Gas-particle partitioning of selected PAHs (mean  $\pm$  sd (median)), observed and  
 344 predicted by the models Junge-Pankow, 1987 (JP), Harner and Bidleman, 1998 (HB), and  
 345 Finizio et al., 1997 (F), expressed as (a) particulate mass fraction,  $\theta$ , and (b) log  $K_p$  of this  
 346 study.

347 a)

	Observed	JP	HB	F
BAA	0.51 $\pm$ 0.28 (0.47)	0.18 $\pm$ 0.07 (0.18)	0.08 – 0.20	0.18
TPH	0.27 $\pm$ 0.13 (0.26)	0.24 $\pm$ 0.10 (0.24)	0.23 – 0.46	0.37
CHR	0.35 $\pm$ 0.15 (0.35)	0.31 $\pm$ 0.13 (0.32)	0.09 – 0.21	0.19
BBF	0.88 $\pm$ 0.40 (0.94)	0.91 $\pm$ 0.40 (0.97)	0.49 – 0.73	0.59

348

349 b)

	Observed	JP	HB	F
BAA	-1.28 ± 1.00 (-0.96)	-1.97 ± 1.14 (-1.84)	-2.43 – -1.98	-1.89
TPH	-1.77 ± 1.27 (1.45)	-1.80 ± 1.07 (-1.63)	-1.91 – -1.46	-1.48
CHR	-1.59 ± 1.18 (1.34)	-1.65 ± 1.01 (-1.46)	-2.41 – -1.96	-1.87
BBF	-0.94 ± 0.19 (-0.24)	-0.52 ± 0.66 (-0.74)	-1.41 – -0.96	-1.08

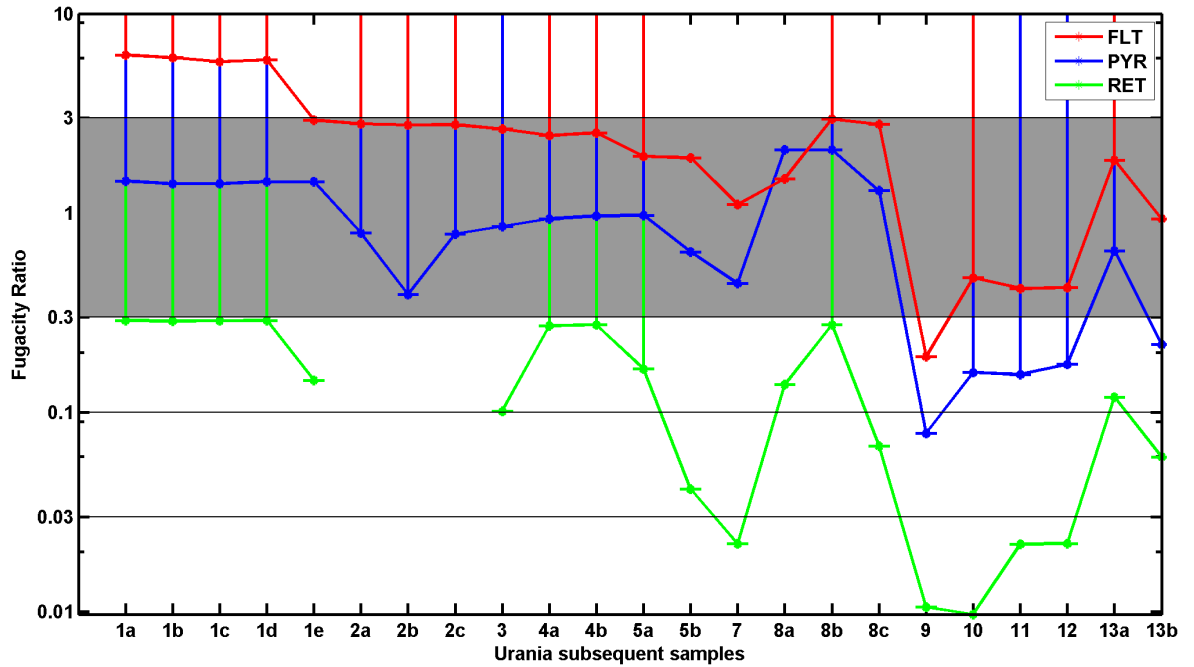
350

### 351 3.3 Fugacity ratio and air-sea exchange flux

352 Fugacity ratios (Fig. 1a) and vertical fluxes (Fig. 1b) could be quantified for FLT, PYR and  
353 RET. The uncertainty window of  $FR = f_a/f_w = 0.3 - 3.0$  is based on the uncertainty of  $H_{Tw,salt}$ .  
354 Values  $FR > 3.0$  indicate net deposition,  $FR < 0.3$  indicate net volatilisation. For RET both  
355 water and air concentrations of sample No. 2 were <LOQ. Transfer coefficients were  $k_w \ll$   
356  $k_a$ .

357 Fig. 1. Air-sea exchange, (a) fugacity ratios  $FR = f_a/f_w$  (volatilisation  $> 3$ , deposition  $< 0.3$ ,  
358 grey area insignificant deviation from phase equilibrium) and (b) flux  $F_{aw}$  ( $ng\ m^{-2}\ d^{-2}$ ;  
359 volatilisation  $> 0$ , deposition  $< 0$ ) of FLT, PYR and RET along the cruise of RV Urania. Error  
360 bars indicate sea water concentration  $C_w < LOQ$ . The x-axis depicts the correspondence of  
361 sequential pairs of air samples (1-13) and water samples (a-e).

362 a.



363

364 b.



365

366

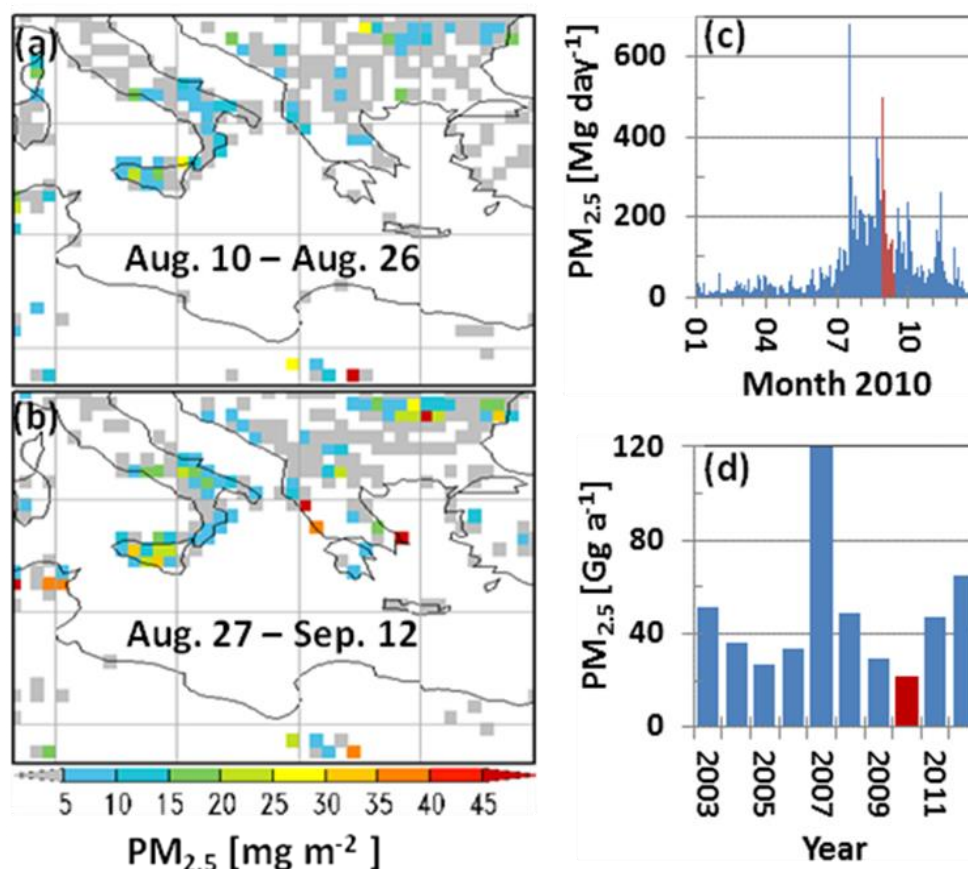
367 FLT and PYR were found to be close to phase equilibrium, with most of the FR values within  
 368 the uncertainty range, one sample (No. 1) indicating deposition of FLT and one or two (No. 9  
 369 and 13) indicating volatilisation of FLT and PYR, respectively. In comparison with earlier

370 observations of FLT and PYR air-sea exchange in the SEM in 2001-02 and 2007 (Tsapakis et  
371 al., 2006; Castro-Jiménez et al., 2012) and considering spatial and temporal variabilities no  
372 trend, in particular no reversal of air-sea exchange is indicated. This comparison is detailed in  
373 the SM, S2.2.1. RET, however, is found net-volatilisation throughout most of the cruise  
374 (Fig. 1). Among the highest fluxes ( $> 50 \text{ ng m}^2 \text{ d}^{-1}$ ) are some samples with very low FR,  
375  $< 0.03$ . Fugacity of RET from water is supported by its Henry's law coefficient ( $11 \text{ Pa m}^3 \text{ mol}^{-1}$   
376  $^1$  at 298 K) which is higher than for CHR ( $0.53 \text{ Pa m}^3 \text{ mol}^{-1}$ ) and FLT ( $2.0 \text{ Pa m}^3 \text{ mol}^{-1}$ ). RET  
377 is commonly considered as biomarker for coniferous wood combustion (Ramdahl, 1983). A  
378 decrease in wildfires could explain the suspected RET volatilisation. Integrated over the  
379 domain and the year 2010, fires released 7.2 PJ fire radiative energy, which translates into  
380 around 22.2 Gg of  $\text{PM}_{2.5}$  emitted (Fig. 2). Compared to the  $\text{PM}_{2.5}$  emissions of the years 2003  
381 to 2012, the year 2010 had the lowest emissions, equivalent to 46% of the 2003-2012 mean,  
382 and only 18% of the peak emissions of the year 2007 (Fig. 2d). As typical for the East  
383 Mediterranean region, the fire season in 2010 started by the end of June and ended by early  
384 October. The Urania cruise measurements took place between 27.8. and 12.9., i.e. towards the  
385 end of the main burning season (Fig. 2c). During the first half of the Urania cruise,  
386 widespread fire activity was observed in the entire domain, with most intense fires occurring  
387 in Southern Italy, Sicilia and along the East coast of the Adriatic and the Ionian Sea (notably  
388 in Albania and Greece) (Fig. 2a).

389

390 Fig. 2. Spatial pattern of fire-related  $\text{PM}_{2.5}$  emissions (Global Fire Assimilation System  
391 GFASv1.0; Kaiser et al., 2012) for the East Mediterranean ( $28-45^\circ\text{N}/8-30^\circ\text{E}$ ), (a) time  
392 integral of August 10-26, (b) time integral of August 27 - September 12, 2010, given as sum

393 over each period in  $\text{mg m}^{-2}$ . Areas with no observed fire activity are displayed in white.  
394 Temporal pattern of domain-integrated (c) daily total  $\text{PM}_{2.5}$  emissions over 2010 (c) and  
395 yearly total  $\text{PM}_{2.5}$  emissions over 2003 to 2012. Labelled in red is (c) the the period of the  
396 Urania cruise (27 August – 11 September 2010) (d) and the year 2010.



397

398

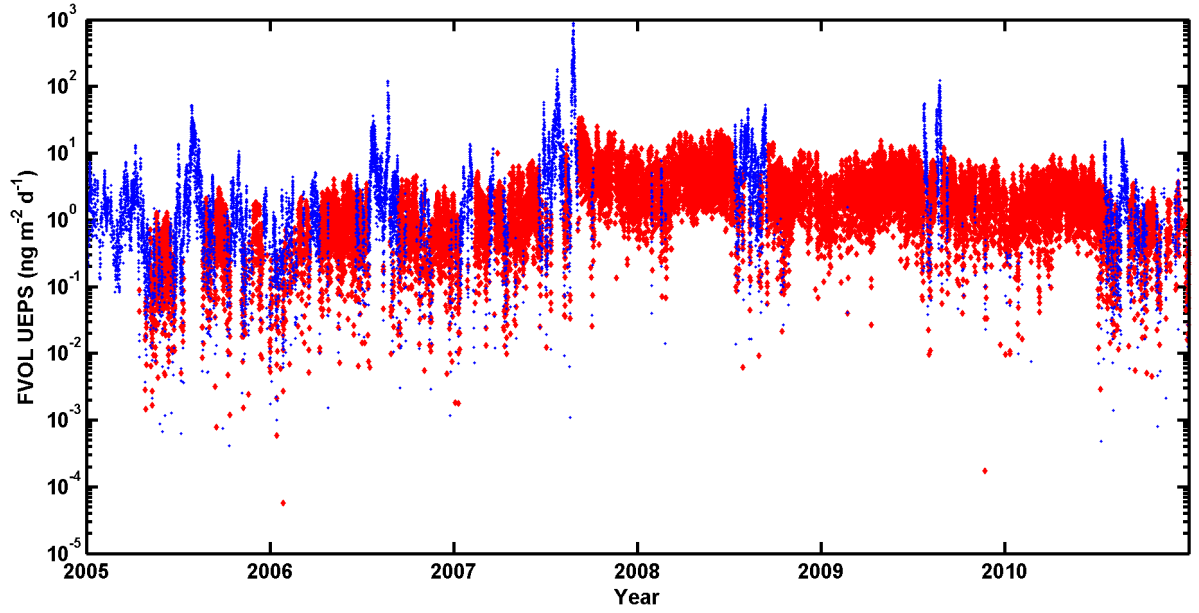
399 The hypothesis that seasonal depositional input of RET into the surface waters during the fire  
400 season (summer) triggers reversal of diffusive air-sea exchange, at least in the year 2010, are  
401 tested by box model (sections 2.5 and S1.3) runs. Two scenarios are considered, an 'Initially  
402 Estimated Parameter Set' (IEPS) representing mean values for environmental parameters, and  
403 an 'Upper Estimate Parameter Set' (UEPS) which represents realistic environmental  
404 conditions favouring seawater pollution (SM, Table S3). Simulated diffusive air-sea exchange

405 flux,  $F_{aw}$ , during 2005-2010 initialised by the UEPS is shown in Fig. 3a and by the IEPS in  
406 the SM, Fig. S3, and during the observations (cruise of RV Urania, 27.8.-9.9.2010) initialised  
407 by the UEPS in Fig. 3b.

408 The model confirms the hypothesis that seasonal depositional input of RET into the surface  
409 waters during the fire season (July-September, typically in the range  $F_{aw} = 10^{-2}$ - $10^1$   $\text{ng m}^{-2} \text{d}^{-1}$   
410 under IEPS) is followed by a period of prevailing flux reversal, typically  $F_{aw} = 10^{-2}$ - $10^0$   $\text{ng m}^{-2}$   
411  $\text{d}^{-1}$ , which in the years 2008-10 started in October and lasted until the onset of the fire  
412 season, but eventually started later in the years 2005-07 (at least under IEPS). The  
413 volatilisation flux is predicted smaller in magnitude than the net-deposition flux during the  
414 fire season, but correspondingly, i.e. higher after intense fire seasons. The high RET  
415 volatilisation flux, indicated by measured  $C_a$  and  $C_w$ , seems to be dominated by biomass  
416 burning in the region in the previous fire season.  $F_{aw}$  is predicted highly fluctuating, also  
417 during the observational period (Fig. 3b). Even under UEPS the model is underpredicting  $F_{aw}$   
418 (Fig. 3b). The sensitivity to input uncertainties (SM S1.2) may explain part of the  
419 underestimate, but not up to one order of magnitude. Neglected RET sources to seawater,  
420 such as riverine input may explain part of the discrepancy.

421

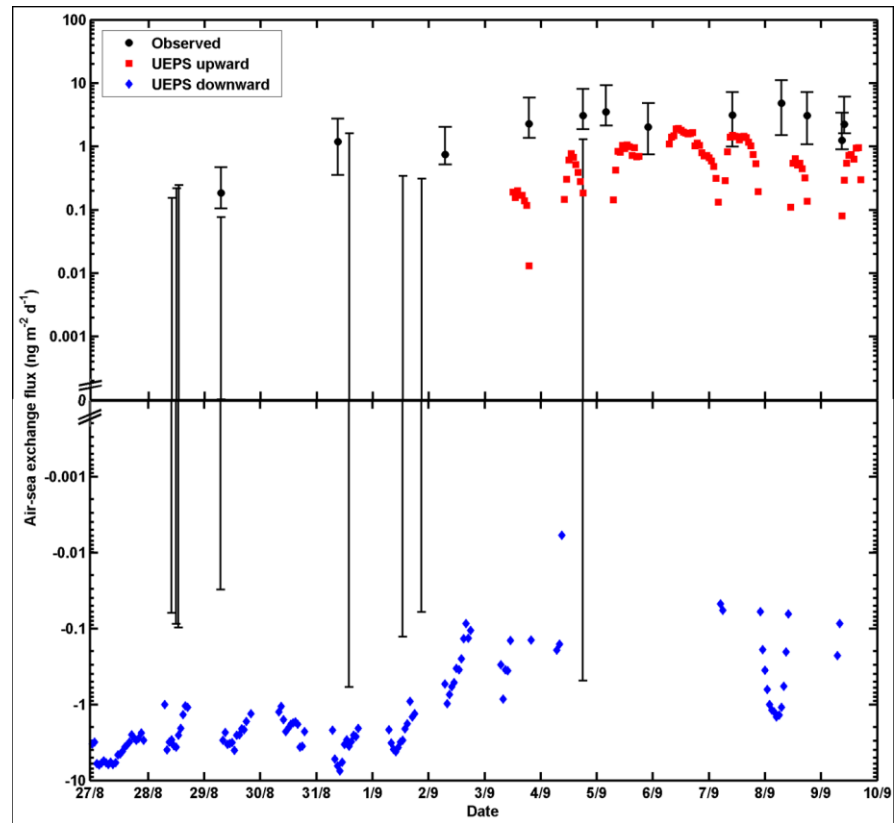
422 Fig. 3. Diffusive air-sea exchange flux,  $F_{aw}$ , of RET ( $\text{ng m}^{-2} \text{d}^{-1}$ ; downward in blue and  
423 upward in red) using the upper estimate parameter set (UEPS) for the Eastern Mediterranean  
424 ( $28$ - $45^\circ\text{N}/8$ - $30^\circ\text{E}$ ) (a.) model predicted for 1.1.2005-31.12.2010 and (b.) model predicted and  
425 observed (black) for 27.8.-9.9.2010. Hourly mean data filtered against off-shore winds (see  
426 text). Error bars including both signs of  $F_{aw}$  reflect  $C_w < \text{LOQ}$ .a.



427

428

429 b.



430

431

432 **4. Conclusions**

433

434 PAH pollution of the atmospheric Mediterranean environment was below previous  
435 observations at the beginning of the decade (2001-02; Tsapakis and Stephanou, 2005a;  
436 Tsapakis et al., 2006), also considering possible losses during sampling. This might reflect  
437 emission reductions. The particulate phase PAHs were concentrated in the size fraction <  
438 0.25  $\mu\text{m}$  a.e.d. The residence time in the troposphere is longest for particles around 0.2  $\mu\text{m}$  of  
439 size, with  $\approx 0.01 \text{ cm s}^{-1}$  being a characteristic corresponding dry deposition velocity (Franklin  
440 et al., 2000), which translates into a residence time of  $\approx 120$  days in the MBL (depth of 1000  
441 m; see Table S3) and deposition flux  $F_{\text{dep}} = c \times v = 0.03\text{-}0.13 \mu\text{g m}^{-2} \text{ year}^{-1}$  for the individual  
442 PAHs associated with the particulate phase ( $c = 0.01\text{-}0.04 \text{ ng m}^{-3}$ ; Table 2b), such as BAP,  
443 and 0.80 and 0.35  $\mu\text{g m}^{-2} \text{ year}^{-1}$ , respectively, for the total flux of particulate phase PAHs in  
444 the ISS and SEM in summer, respectively. The flux will be higher in winter, because of the  
445 seasonality of the emissions.

446 Three gas-particle partitioning models were tested and found to underpredict the particulate  
447 mass fraction in most of the samples (four PAHs i.e., BAA, TPH, CHR and BBF). Although  
448 input parameters were incomplete these results confirm the earlier insight that additional  
449 processes on the molecular level need to be included, beyond adsorption (Junge-Pankow  
450 model) and absorption in OM ( $K_{\text{oa}}$  models), namely both adsorption and absorption  
451 (Lohmann and Lammel, 2004) or even a complete description of molecular interactions  
452 between sorbate and PM matrix (Goss and Schwarzenbach, 2001).

453 Simulations with a non-steady state 2-box model confirm the hypothesis that seasonal  
454 depositional input of RET from biomass burning into the surface waters during summer is  
455 followed by a period of flux reversal. The volatilisation flux is smaller in magnitude than the

456 net-deposition flux during the previous months, but correspondingly, i.e. higher after intense  
457 fire seasons. Future negative emission trends or interannual variability of regional sources  
458 may trigger the sea to become a secondary PAH source through reversal of diffusive air-sea  
459 exchange. For the wood burning marker RET it is found that the secondary source became  
460 significant in recent years: While the flux of secondary RET emissions (from surface  
461 seawaters) in the study area was  $1.0 \mu\text{g m}^{-2} \text{ year}^{-1}$  (mean of years 2005-2010,\_UEPS), the  
462 primary sources amounted to  $3.1 \mu\text{g m}^{-2} \text{ year}^{-1}$ . Because of non-diffusive emission from the  
463 sea surface, such as aerosol suspension from sea spray and bubble bursting (Woolf, 1997;  
464 Qureshi et al., 2009; Albert et al., 2012), the true volatilisation may have exceeded the  
465 diffusive flux significantly.

466

#### 467 **Acknowledgements**

468 We thank the crew of RV Urania for scientific support during the cruise, and Giorgos  
469 Kouvarakis and Nikolas Mihalopoulos, University of Crete, Franz Meixner, MPIC, and  
470 Manolios Tsapakis, HCMR Gournes-Pediados, for discussion and providing meteorological  
471 data. This research was supported by the Granting Agency of the Czech Republic (GACR  
472 project No. P503/11/1230), by the European Commission (European Structural Funds project  
473 No. CZ.1.05/2.1.00/01.0001, CETOCOEN) and has been co-funded from the European  
474 Social Fund and the state budget of the Czech Republic.

475

#### 476 **References**

- 477 Albert, M.F.M.A., Schaap, M., Manders, A.M.M., Scannell, C., O'Dowd, C.D., de Leeuw, G.:  
478       Uncertainties in the determination of global sub-micron marine organic matter emissions,  
479       *Atmos. Environ.*, 2012, 57, 289-300.
- 480 Akyüz, M., Çabuk, H.: Gas-particle partitioning and seasonal variation of polycyclic aromatic  
481       hydrocarbons in the atmosphere of Zonguldak, Turkey. *Sci. Total Environ.*, 2010, 408,  
482       5550-5558.
- 483 Balasubramanian, R., He, J.: Fate and transfer of persistent organic pollutants in a multimedia  
484       environment. In: Zereini, F., Wiseman, C.L.S. (eds) *Urban airborne particulate matter: origins, chemistry, fate and health impacts*. Springer, Heidelberg, pp. 277-307, 2010.
- 485

486 Berrojalbiz, N., Dachs, J., Ojeda, M.J., Valle, M.C., Castro Jiménez, J., Wollgast, J., Ghiani,  
487 M., Hanke, G., Zaldivar, J.M.: Biogeochemical and physical controls on concentrations of  
488 polycyclic aromatic hydrocarbons in water and plankton of the Mediterranean and Black  
489 Seas, *Glob. Biogeochem. Cycles*, 2011, 25, GB4003.

490 Bidleman, T.F., McConnell, L.L.: A review of field experiments to determine air–water gas-  
491 exchange of persistent organic pollutants. *Sci. Total Environ.*, 1995, 159, 101-107.

492 Bruhn, R., Lakaschus, S., McLachlan, M.S.: Air/sea gas exchange of PCBs in the southern  
493 Baltic sea. *Atmos. Environ.*, 2003, 37, 3445–3454.

494 Castro-Jiménez, J., Berrojalbiz, N., Wollgast, J., Dachs, J.: Polycyclic aromatic hydrocarbons  
495 (PAHs) in the Mediterranean Sea: Atmospheric occurrence, deposition and decoupling  
496 with settling fluxes in the water column. *Environ. Pollut.*, 2012, 166, 40-47.

497 Chrysikou, L.P., Gemenetzi, P.G., Samara, C.A.: Wintertime size distributions of polycyclic  
498 aromatic hydrocarbons (PAH), polychlorinated biphenyls (PCB) and organochlorine  
499 pesticides (OCPs) in the urban environment: Street- vs. rooftop-level measurements.  
500 *Atmos. Environ.*, 2009, 43, 290-300.

501 Dachs, J., Bayona, J.M., Raoux, C., Albaiges, J.: Spatial, vertical distribution and budget of  
502 polycyclic aromatic hydrocarbons in the western Mediterranean seawater. *Environ. Sci.  
503 Technol.*, 1997, 31, 682-688.

504 Dvorská, A., Lammel, G., Klánová, J.: Use of diagnostic ratios for studying source  
505 apportionment and reactivity of ambient polycyclic aromatic hydrocarbons over central  
506 Europe. *Atmos. Environ.*, 2011, 45, 420-427.

507 Eckhardt, S., Breivik, K., Manø, S., Stohl, A.: Record high peaks in PCB concentrations in  
508 the Arctic atmosphere due to long-range transport of biomass burning emissions, *Atmos.  
509 Chem. Phys.*, 2007, 7, 4527–4536.

510 Finizio, A., Mackay, D., Bidleman, T.F., Harner, T.: Octanol-air partition coefficient as a  
511 predictor of partitioning of semi-volatile organic chemicals to aerosols. *Atmos. Environ.*,  
512 1997, 31, 2289-2296.

513 Franklin, J., Atkinson, R., Howard, P.H., Orlando, J.J., Seigneur, C., Wallington, T.J.,  
514 Zetzsch, C.: Quantitative determination of persistence in air. In: *Criteria for persistence  
515 and long-range transport of chemicals in the environment* (Klečka, G., Boethling, B.,

516 Franklin, J., Grady, L., Graham, D., Howard, P.H., Kannan, K., Larson, R.J., Mackay, D.,  
517 Muir, D., van de Meent, D., eds.), SETAC Press, Pensacola, USA, pp. 7-62, 2000.

518 Galarneau, E., Bidleman, T.F., Blanchard, P.: Modelling the temperature-induced blow-off  
519 and blow-on artefacts in filter-sorbent measurements of semivolatile substances. *Atmos.*  
520 *Environ.*, 2006, 40, 4258-4268.

521 Goss, K.U., Schwarzenbach, R.P.: Linear free energy relationships used to evaluate  
522 equilibrium partitioning of organic compounds. *Environ. Sci. Technol.*, 2001, 35, 1–9.

523 Greenfield, B.K., Davis, J.A.: A PAH fate model for San Francisco Bay, *Chemosphere*, 2005,  
524 6, 515-530.

525 Guitart, C., Garcá-Flor, N., Miquel, J.C., Fowler, S.W., Albaiges, J.: Effect of accumulation  
526 PAHs in the sea surface microlayer on their coastal air-sea exchange, *J. Mar. Systems*,  
527 2010, 79, 210-217

528 Harner, T., Bidleman, T.F.: Octanol–air partition coefficient for describing particle-gas  
529 partitioning of aromatic compounds in urban air. *Environ Sci Technol.*, 1998, 32, 1494 –  
530 1502.

531 Hoff, E.M., Brice, K.A., Halsall, C.J.: Non-linearities in the slope of Clausius-Clapeyron  
532 plots for semivolatile organic compounds. *Environ. Sci. Technol.*, 1998, 32, 1793–1798.

533 Jaenicke, R.: Aerosol physics and chemistry. In: *Numerical Data and Functional*  
534 *Relationships in Science and Technology*, ed. G. Fischer, vol. 4, pp. 391-457, Springer,  
535 Berlin, 1988.

536 Kaiser, J.W., Heil, A., Andreae, M.O., Benedetti, A., Chubarova, N., Jones, L., Morcrette, J.J.,  
537 Razinger, M., Schultz, M.G., Suttie, M., van der Werf, G.R.: Biomass burning emissions  
538 estimated with a global fire assimilation system based on observed fire radiative power.  
539 *Biogeosci.*, 2012, 9, 527-554.

540 Karickhoff, S.W.: Semiempirical estimation of sorption of hydrophobic pollutants on natural  
541 sediments and soils. *Chemosphere*, 1981, 10, 833-849.

542 Kavouras, I.G., Stephanou, E.G.: Particle size distribution of organic primary and secondary  
543 aerosol constituents in urban, background marine, and forest atmosphere. *J. Geophys.*  
544 *Res.*, 2002, 107, 4069.

545 Keyte, I.J., Harrison, R.M., Lammel, G.: Chemical reactivity and long-range transport  
546 potential of polycyclic aromatic hydrocarbons – a review, *Chem. Soc. Rev.*, 2013, 42,  
547 9333-9391.

548 Kiss, G., Varga-Puchony, Z., Rohrbacher, G., Hlavay, J.: Distribution of polycyclic aromatic  
549 hydrocarbons on atmospheric aerosol particles of different sizes, *Atmos. Res.*, 1998, 46,  
550 253-261.

551 Lammel, G.: Effects of time-averaging climate parameters on predicted multicompartmental  
552 fate of pesticides and POPs. *Environ. Pollut.*, 2004, 128, 291-302.

553 Lammel, G., Sehili, A.M., Bond, T.C., Feichter, J., Grassl, H.: Gas/particle partitioning and  
554 global distribution of polycyclic aromatic hydrocarbons – a modelling approach.  
555 *Chemosphere*, 2009a, 76, 98-106.

556 Lammel, G., Klánová, J., Kohoutek, J., Prokeš, R., Ries, L., Stohl, A.: Observation and origin  
557 of organochlorine pesticides, polychlorinated biphenyls and polycyclic aromatic  
558 hydrocarbons in the free troposphere over central Europe. *Environ. Pollut.*, 2009b, 157,  
559 3264-3271.

560 Lammel G., Klánová J., Ilić P., Kohoutek J., Gasić B., Kovacić I., Lakić N., Radić R.:  
561 Polycyclic aromatic hydrocarbons on small spatial and temporal scales – I. Levels and  
562 variabilities, *Atmos. Environ.*, 2010a, 44, 5015-5021.

563 Lammel, G., Klánová, J., Ilić, P., Kohoutek, J., Gasić, B., Kovacić, I., Škrdlíková, L.:  
564 Polycyclic aromatic hydrocarbons on small spatial and temporal scales – II. Mass size  
565 distributions and gas-particle partitioning, *Atmos. Environ.*, 2010b, 44, 5022-5027.

566 Lammel, G., Novák, J., Landlová, L., Dvorská, A., Klánová, J., Čupr, P., Kohoutek, J.,  
567 Reimer, E., Škrdlíková, L.: Sources and distributions of polycyclic aromatic hydrocarbons  
568 and toxicity of polluted atmosphere aerosols. In: *Urban Airborne Particulate Matter:  
569 Origins. Chemistry. Fate and Health Impacts* (Zereini. F., Wiseman. C.L.S., eds.),  
570 Springer, Berlin, pp. 39-62, 2010c.

571 Lei, Y.D., Chankalal, R., Chan, A., Wania, F.: Supercooled liquid vapor pressures of the  
572 polycyclic aromatic hydrocarbons. *J. Chem. Eng. Data*, 2002, 47, 801–806.

573 Lim, L., Wurl, O., Karuppiyah, S., Obbard, J.P.: Atmospheric wet deposition of PAHs to the  
574 sea-surface microlayer, *Mar. Poll. Bull.*, 2007, 54, 1212-1219.

575 Lippiatou, E., Saliot, A.: Fluxes and transport of anthropogenic and natural polycyclic  
576 aromatic-hydrocarbons in the western Mediterranean Sea. *Mar. Chem.*, 1991, 32, 51-71.

577 Lippiatou, E., Tolosa, I., Simó, R., Bouloubassi, I., Dachs, J., Marti, S., Sicre, M.A., Bayona,  
578 J.M., Grimalt, J.O., Saliot, A., Albaiges J.: Mass budget and dynamics of polycyclic  
579 aromatic hydrocarbons in the Mediterranean Sea, *Deep Sea Res. II*, 1997, 44, 881-905.

580 Liss, P.S., Slater, P.G.: Flux of gases across air-sea interface. *Nature*, 1974, 247, 181-184.

581 Lohmann, R., Lammel G.: Adsorptive and absorptive contributions to the gas particle  
582 partitioning of polycyclic aromatic hydrocarbons: State of knowledge and recommended  
583 parameterization for modelling. *Environ. Sci. Technol.*, 2004, 38, 3793-3803.

584 Lohmann, R., Dapsis, M., Morgan, E.J., Dekany, E., Luey, P.J.: Determining airwater  
585 exchange spatial and temporal trends of freely dissolved PAHs in an urban estuary using  
586 passive polyethylene samplers. *Environ. Sci. Technol.*, 2011, 45, 2655-2662.

587 Lüers, F., ten Hulscher, T.E.M.: Temperature effect on the partitioning of polycyclic aromatic  
588 hydrocarbons between natural organic carbon and water. *Chemosphere*, 1996, 33, 643-  
589 657.

590 Ma, Y.G., Lei, Y.D., Xiao, H., Wania, F., Wang, W.H.: Critical review and recommended  
591 values for the physical-chemical property data of 15 polycyclic aromatic hydrocarbons at  
592 25°C. *J. Chem. Eng. Data*, 2010, 55, 819-825

593 Mai, C.: Atmospheric deposition of organic contaminants into the North Sea and the western  
594 Baltic Sea, PhD thesis, University of Hamburg, Hamburg, Germany, 444 pp., URL:  
595 [http://www.chemie.uni-hamburg.de/bibliothek/diss2012\\_/DissertationMai.pdf](http://www.chemie.uni-hamburg.de/bibliothek/diss2012_/DissertationMai.pdf), 2012.

596 Mandalakis, M., Tsapakis, M., Tsoga, A., Stephanou, E.G.: Gas-particle concentrations and  
597 distribution of aliphatic hydrocarbons, PAHs, PCBs and PCDD/Fs in the atmosphere of  
598 Athens (Greece). *Atmos. Environ.*, 2002, 36, 4023-4035.

599 Masclet, P., Pistikopoulos, P., Beyne, S., Mouvier, G. : Long range transport and gas/particle  
600 distribution of polycyclic aromatic hydrocarbons at a remote site in the Mediterranean  
601 Sea, *Atmos. Environ.*, 1988, 22, 639-650.

602 Pankow, J.F.: Review and comparative analysis of the theory of partitioning between the  
603 gas and aerosol particulate phases in the atmosphere. *Atmos. Environ.*, 1987, 21, 2275-  
604 2283.

605 Pankow, J.F., Bidleman, T.F.: Interdependence of the slopes and intercepts from log-log  
606 correlations of measured gas-particle partitioning and vapor pressure. I. Theory and  
607 analysis of available data. *Atmos. Environ.*, 1992, 26A, 1071-1080.

608 Pujo-Pay, M., Conan, P., Oriol, L., Cornet-Barthaux, V., Falco, C., Ghiglione, J.F., Goyet, C.,  
609 Moutin, T., Prieur, L.: Integrated survey of elemental stoichiometry (C, N, P) from the  
610 western to eastern Mediterranean Sea. *Biogeosci.*, 2011, 8, 883-899.

611 Rowe, C.L., Mitchelmore, C.L., Baker, J.E.: Lack of biological effects of water  
612 accommodated fractions of chemically-and physically-dispersed oil on molecular,  
613 physiological, and behavioral traits of juvenile snapping turtles following embryonic  
614 exposure. *Sci. Total Environ.*, 2009, 407, 5344-5355.

615 Putaud, J.P., Raes, F., van Dingenen, R., Brüggemann, E., Facchini, M.C., Decesari, S.,  
616 Fuzzi, S., Gehrig, R., Hüglin, C., Laj, P., Lorbeer, G., Maenhaut, W., Mihalopoulos, N.,  
617 Müller, K., Querol, X., Rodriguez, S., Schneider, J., Spindler, G., ten Brink, H., Tørseth,  
618 K., Wiedensohler, A.: A European aerosol phenomenology-2: chemical characteristics of  
619 particulate matter at kerbside, urban, rural and background sites in Europe. *Atmos.*  
620 *Environ.*, 2004, 38, 2579–2595.

621 Qureshi, A., MacLeod, M., Hungerbühler, K.: Modeling aerosol suspension from soils and  
622 oceans as sources of micropollutants to air, *Chemosphere*, 2009, 77, 495-500.

623 Ramdahl, T.: Retene — a molecular marker of wood combustion in ambient air. *Nature*,  
624 1983, 306, 580 - 582.

625 Schmidl, C., Bauer, H., Dattler, A., Hitzenberger, R., Weissenböck, G.: Chemical  
626 characterisation of particle emissions from burning leaves. *Atmos. Environ.*, 2008, 42,  
627 9070–9079.

628 Schnelle, J., Jänsch, J., Wolf, K., Gebefügi, I., Kettrup, A.: Particle size dependent  
629 concentrations of polycyclic aromatic hydrocarbons (PAH) in the outdoor air.  
630 *Chemosphere*, 1995, 31, 3119-3127.

631 Schwarzenbach, R.P., Gschwend, P.M. Imboden, D.M.: *Environmental Organic Chemistry*.  
632 2nd ed., Wiley, Hoboken, USA, 2003.

633 Spindler, G., Gnauk, T., Grüner, A., Iinuma, Y., Müller, K., Scheinhardt, S., Herrmann, H.:  
634 Site-segregated characterization of PM<sub>10</sub> at the EMEP site Melpitz (Germany) using a  
635 five-stage impactor: a six year study. *J. Atmos. Chem.*, 2012, 69, 127-157.

636 Stohl, A., Hitzenberger, M., Wotawa, G.: Validation of the Lagrangian particle dispersion  
637 model FLEXPART against large scale tracer experiments. *Atmos. Environ.*, 1998, 32,  
638 4245-4264.

639 Stohl, A., Forster, C., Eckhardt, S., Spichtinger, N., Huntrieser, H., Heland, J., Schlager,  
640 H., Wilhelm, S., Arnold, F., Cooper, O.: A backward modeling study of intercontinental  
641 pollution transport using aircraft measurements. *J. Geophys. Res.*, 2003, 108, 4370,  
642 doi:10.1029/2002jd002862.

643 Stohl, A., Forster, C., Frank, A., Seibert, P., Wotawa, G.: Technical Note: The Lagrangian  
644 particle dispersion model FLEXPART version 6.2. *Atmos. Chem. Phys.*, 2005, 5, 2461-  
645 2474.

646 Tsapakis, M., Stephanou, E.G.: Collection of gas and particle semi-volatile organic  
647 compounds: Use of an oxidant denuder to minimize polycyclic aromatic hydrocarbons  
648 degradation during high-volume air sampling. *Atmos. Environ.*, 2003, 37, 4935-4944.

649 Tsapakis, M., Stephanou, E.G.: Polycyclic aromatic hydrocarbons in the atmosphere of the  
650 Eastern Mediterranean. *Environ. Sci. Technol.*, 2005a, 39, 6584-6590.

651 Tsapakis, M., Stephanou, E.G.: Occurrence of gaseous and particulate polycyclic aromatic  
652 hydrocarbons in the urban atmosphere: study of sources and ambient temperature effect  
653 on the gas/particle concentration and distribution. *Environ. Poll.*, 2005b, 133, 147-156.

654 Tsapakis, M., Stephanou, E.G., Karakassis, I.: Evaluation of atmospheric transport as a non-  
655 point source of polycyclic aromatic hydrocarbons in marine sediments of the Eastern  
656 Mediterranean, *Mar. Chem.*, 2003, 80, 283-298.

657 Tsapakis, M., Apsotolaki, M., Eisenreich, S., Stephanou, E.G.: Atmospheric deposition and  
658 marine sedimentation fluxes of polycyclic aromatic hydrocarbons in the Eastern  
659 Mediterranean Basin, *Environ. Sci. Technol.*, 2006, 40, 4922-4927.

660 Woolf, D.K.: Bubbles and their role in gas exchange, in: *Sea Surface and Global Change*  
661 (Liss, P.S., Duce, R.A., eds.), Cambridge University Press, Cambridge, UK, pp. 173-206,  
662 1997.

663 Zhong, G., Xie, Z., Möller, A., Halsall, C., Caba, A., Sturm, R., Tang, J., Zhang, G.,  
664 Ebinghaus, R.: Currently used pesticides, hexachlorobenzene and  
665 hexachlorocyclohexanes in the air and seawater of the German Bight (North Sea).  
666 Environ. Chem., 2012, 9, 405-414.  
667